Case study of proppant selection for a Montney well using discrete element simulations

Wenbo Zheng, University of British Columbia
Dwayne Tannant, University of British Columbia

Summary

The high closure stress acting on proppants within hydraulic fractures often crushes proppant grains into smaller fragments (Palisch et al. 2009). For example, crushed sand was observed in flow back tests from Montney formation under a closure stress of 42.3 MPa (Romanson et al. 2010). Under such a high closure stress between the newly created fractures, another important issue affecting the fracture conductivity is proppant embedment into rock fracture surfaces. Laboratory testing performed using mesh 40/70 Badger sand proppants sandwiched between two Barnett shale cores found that half of the proppant grains were embedded into each shale core under a compression stress of 27.6 MPa (Zhang et al. 2015). Proppant crushing and embedment allows hydraulic fractures to close thus reducing the fracture aperture. Furthermore, the presence of small fragments of crushed sand decreases the permeability or hydraulic conductivity of the proppant pack because they can block natural gas flow paths.

Careful selection of proppant types and size are required to maintain the conductivity of hydraulic fractures after hydraulic fracturing and the selection should be tailored to the specific reservoir geomechanical properties. As an alternate to costly laboratory proppant testing, the discrete element method (DEM) has been used to study proppant embedment into fractures (Deng et al. 2014, Zhang et al. 2017). DEM modeling of proppants was further improved by the authors to incorporate a particle breakage model to simulate particle fragmentation during proppant crushing (Zheng and Tannant 2018). The simulated geometry of proppants between fractures can be used to obtain the conductivity of proppant packs by using empirical Kozeny-Carman equation (Zheng and Tannant 2017) or flow simulations (Fan et al. 2018).

In this paper, the 3D DEM simulations were used to study the proppant selection for a well in Montney Formation. This well has a closure stress of 27.6 MPa and the rock properties were obtained through rock mechanics testing. Proppant crushing and embedment between rock fractures were modeled at the stress of 27.6 and the change in fracture aperture and proppant grain sizes were captured. The grain size distribution of proppants was used to estimate the permeability of proppants. The permeability was multiplied by the fracture aperture to give the propped fracture conductivity. Five different scenarios of proppant selection were simulated, and the resulting fracture conductivity was used in comparison of Return-on-Fracturing-Investment (ROFI) for different proppant selection.

Method

The horizontal well was drilled at a depth of around 2258 m (TVD) and the total length is about 2 km. Hydraulic fracturing was conducted with 35 perforation clusters along the horizontal portion of the well. Three types of proppant were used at each stimulation stage of the well. Proppant 1 is a mesh 50/140 sand mainly for fluid leak off control, Proppant 2 is a mesh 40/70 sand, and Proppant 3 is a mesh 20/40 resin coated sand that can bond the proppant pack to control proppant flowback. The mass ratio of Proppant 1 to Proppant 2 to Proppant is 1:25:5 for stages from #2 to #9. Assuming the mechanical

properties of Proppant 1 and Proppant 2 are similar to Jordan sand, and those of Proppant 3 are similar to the resin-coated sand.

To calculate the average fracture conductivity provided by the proppant pack, proppant pack was assumed to have uniform thickness/concentration on a cross-section perpendicular to the minimum horizontal stress. The fracture conductivity provided by the average proppant concentration was determined from a DEM simulation. As shown in Figure 1, the proppant mixture was placed between two rock faces and compressed to 27.5 MPa. Proppant grains were simulated with DEM particles (blue) and the rock formation was represented with DEM particles (orange) bonded to each other. Proppant embedment into rock can be captured through the interaction of DEM elements at the particle scale. Proppant particles were allowed to break once they reach their crushing threshold, which was implemented through a breakage model in DEM. The aperture between the two rock faces was obtained directly from the DEM simulation. The particle size distribution of proppant after loading to 27.5 MPa was used to calculate the proppant pack permeability via the empirical Kozeny-Carman equation. Multiplying the permeability by the fracture apertures gives the fracture conductivity.
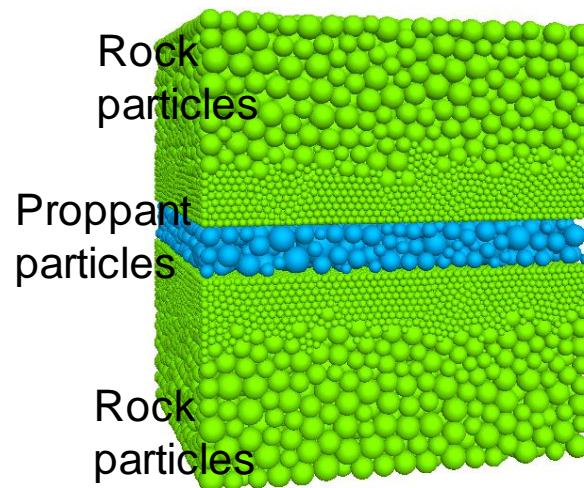
Figure 1. Proppants compressed between two rock faces

Results and Conclusions

Several scenarios of proppant selection were simulated in DEM and the resulting proppant pack permeability and fracture conductivity are summarized in Table 1. To evaluate the impact of proppant selection in hydraulic fracturing treatments on the economics of the well production, the Return-On-Fracturing-Investment (ROFI) after a 1-year production was calculated as the total gas production value after 1-year production subtracted by the proppant cost and non-proppant hydraulic fracturing cost. The gas production after one year was assumed proportional to the square root of the propped fracture conductivity. The values of the proppant cost and non-proppant cost were used to calculate the completion cost of the investigated well. The price of the resin-coated sand is assumed to be $540/tonne, 3 times of that of regular frac sand.
The calculated ROFI for the base scenario is 0.03 million dollars.

Table 1. Different proppant selection scenarios and resulting ROFIs after 1-year production

Scenario	Base	1	2	3	4
Proppant type	50/140 sand, 40/70 sand, 20/40 resin-coated sand	50/140 sand, G600 sand, 20/40 resin-coated sand	50/140 sand, G300 sand, 20/40 resin-coated sand	50/140 sand, G300 sand, 30/50 resin-coated sand	50/140 sand, G300 sand
Total proppant usage in tonne (mass ratio)	1080 (1:25:5)	1080 (1:25:5)	1080 (1:25:5)	1080 (1:25:5)	1080 (1:30)
fluid (m^3)	9723.5	9723.5	9723.5	9723.5	9723.5
Fracture aperture (mm)	0.689	0.654	0.718	0.727	0.738
Void ratio	0.674	0.591	0.744	0.765	0.792
Effective diameter (mm)	0.300	0.410	0.336	0.326	0.314
Permeability (μm^2)	90.8	121.4	149.0	150.0	152.0
Fracture conductivity (μm^3)	63000	80000	108000	110000	114000
Production after 1 year (million m^3)	11.8	13.3	15.4	15.5	15.8
Production value (million $)	1.84	2.07	2.40	2.42	2.46
Proppant cost (million $)	0.26	0.26	0.26	0.26	0.16
Non-proppant cost (million $)	1.56	1.56	1.56	1.56	1.56
ROFI (million $)	0.03	0.25	0.59	0.61	0.74

The results show that Scenario 2, 3 and 4 can significantly improve the hydrocarbon production and thus the ROFIs at 1 year. Scenario 4 gives the highest ROFI of 0.74 million dollars due to the lowest cost for the proppant when not using the expensive resin-coated sand. When proppant flow back is considered, Scenario 3 with the resulting ROFI 0.61 million dollars should be used. In addition, the mesh 30/50 resin-coated sand in Scenario 3 has better transport capacity than the larger mesh size 20/40 used in the base case.

References

1. Palisch, T. T., Duenckel, R. J., Chapman, M. A. et al. 2009. How to use and misuse proppant crush tests - exposing the top 10 myths. SPE Hydraulic Fracturing Technology Conference, The Woodlands, 19-21 January. SPE-119242-MS.
2. Romanson, R., Riviere, N., Taylor, B. et al. 2010. Montney fracturing-fluid considerations: case history. Canadian Unconventional Resources and International Petroleum Conference, Society of Petroleum Engineers.
3. Zhang, J., Ouyang, L., Zhu, D. et al. 2015. Experimental and numerical studies of reduced fracture conductivity due to proppant embedment in the shale reservoir. Journal of Petroleum Science and Engineering, 130: 37-45.
4. Deng, S., Li, H., Ma, G. et al. 2014. Simulation of shale-proppant interaction in hydraulic fracturing by the discrete element method. International Journal of Rock Mechanics & Mining Sciences, 70: 219–228.
5. Zhang, F., Zhu, H., Zhou, H. et al. 2017. Discrete-element-method/computational-fluid-dynamics coupling simulation of proppant embedment and fracture conductivity after hydraulic fracturing. SPE Journal, 22(02): SPE-185172-PA.
6. Zheng, W. and Tannant D. D. 2018. grain breakage criteria for discrete element models of sand crushing under one-dimensional compression. Computers & Geotechnics, 95: 231-239.
7. Zheng, W. and Tannant, D. D. 2017. Improved estimate of the effective diameter for use in the kozeny-carman equation for permeability prediction. Géotechnique Letters, 7(1):1-5.
8. Fan, M., McClure, J., Han, Y. et al. 2018. Interaction between proppant compaction and single-/multiphase flows in a hydraulic fracture. SPE Journal. SPE-189985-PA.